Histol Histopathol (2023) 38: 681-693

https://www.hh.um.es

Histology and Histopathology
From Cell Biology to Tissue Engineering

ORIGINAL ARTICLE **Open Access**

Circ_0079530 stimulates THBS2 to promote the malignant progression of non-small cell lung cancer by sponging miR-584-5p

Kun Fang[1], Yibin Deng[2], Ping Yang[1], Yurong Zhang[1], Dan Luo[3], Fang Wang[1], Zhilong Cai[1] and Yang Liu[1]

[1]Department of Clinical Laboratory, [2]Department of Pediatric and [3]Department of Gynaecology and Obstetrics (Science and Education Department), Sichuan Science City Hospital, Mianyang, PR China

Summary. Background. Circ_0079530 has been confirmed to be a novel potential oncogene in non-small cell lung cancer (NSCLC). This study aims to explore the role and mechanism of circ_0079530 in NSCLC progression.

Methods. Levels of circ_0079530, microRNA (miR)-584-5p, thrombospondin-2 (THBS2), PCNA, Bax, E-cadherin, and ki67 were detected by quantitative real-time PCR (qRT-PCR), western blotting and immunohistochemistry. The proliferation of NSCLC cells was measured using cell counting kit 8 (CCK8) assay, colony formation assay, and EdU staining. Cell apoptosis and motility were respectively detected by flow cytometry and transwell assays. Interaction between miR-584-5p and circ_0079530 or THBS2 was predicted by bioinformatics analysis and confirmed via luciferase reporter assay and RNA immunoprecipitation (RIP) assay. A xenograft tumor model was used to analyze the role of circ_0079530 in tumor growth *in vivo*.

Results. Circ_0079530 was highly expressed in NSCLC tissues and cell lines. Circ_0079530 overexpression facilitated proliferation, migration, and invasion whereas it restrained the apoptosis of NSCLC cells. Circ_0079530 silence showed the opposite effects on the above malignant biological behaviors. Mechanistic analysis showed that circ_0079530 functioned as a sponge of miR-584-5p to relieve the suppressive action of miR-584-5p on its target THBS2. Additionally, circ_0079530 knockdown impeded the growth of xenografts *in vivo*.

Conclusion. Circ_0079530 promoted NSCLC progression by regulating the miR-584-5p/THBS2 axis, providing a possible circRNA-targeted therapy for NSCLC.

Corresponding Author: Yang Liu, Department of Clinical Laboratory, Sichuan Science City Hospital, No. 64 Mianshan Road, Youxian District, Mianyang 621900, PR China. e-mail: lyyang0103@163.com

DOI: 10.14670/HH-18-545

Key words: NSCLC, circ_0079530, miR-584-5p, THBS2

Introduction

Lung cancer is one of the main killers of cancer-associated death worldwide, and high morbidity and high mortality are its important characteristics (Bray et al., 2018). The cases of non-small cell lung cancer (NSCLC) account for about 85% of lung cancer cases (Siegel et al., 2018). At present, the main treatment for NSCLC is a combination of surgical resection and chemotherapy (Duma et al., 2019; Yang et al., 2020). However, due to late diagnosis, metastasis and recurrence, and imperfect development of molecularly targeted drugs, the prognosis of many patients is still unsatisfactory (Gridelli et al., 2015; Lee et al., 2018). Therefore, in-depth exploration and study of the pathophysiological mechanism of NSCLC, and the further development of NSCLC molecular targeted therapeutic drugs with higher targeting and better safety is urgent.

Circular RNA (circRNA) is a conserved endogenous non-coding RNA molecule. The special circular structure of circRNA makes it resistant to RNase-mediated degradation and maintains structural stability, so it is used as a diagnostic or therapeutic biomarker for cancers (Santer et al., 2019; Qin et al., 2020). More and more experiments have shown that circRNA plays an important role in malignant cancers including NSCLC (Li and Han, 2019; Papatsirou et al., 2021). For example, circ-LDLRAD3 has been proven to contribute to the progression of NSCLC by the miR-137/SLC1A5 axis (Xue et al., 2020). It is worth noting that circ_0079530, a newly discovered circRNA, was first confirmed to be upregulated in NSCLC tissue samples and cells. Furthermore, a series of experimental results show that knockdown circ_0079530 can significantly inhibit the growth and motility of NSCLC cells (Li et al., 2018).

However, the detailed mechanism of circ_0079530 in the development of NSCLC has not been reported yet.

MicroRNA (miRNA), another non-coding RNA containing 18-24 nucleotides, is usually negatively regulated by circRNA through the endogenous competitive RNA (ceRNA) mechanism (Panda, 2018; Zhong et al., 2018). That circRNA indirectly regulates the mRNA expression of downstream target genes and affects the function of NSCLC cells through sponging miRNA has been reported many times (Liang et al., 2020). For example, circ_0001869 promotes FOSL2 expression by sponging miR-638 in NSCLC cells (Xu et al., 2020). Also, circ-ZKSCAN1 contributes to FAM83A-mediated NSCLC malignant progression via targeting miR-330-5p (Wang et al., 2019). In addition, the results of bioinformatics analysis predict that there are targeted binding sites for circ_0079530 and thrombospondin-2 (THBS2) on the miR-584 sequence. Meanwhile, Lee et al. have confirmed that miR-584-5p suppressed NSCLC cell growth by inhibiting the level of YKT6 protein *in vivo* and *in vitro* experiments (Lee et al., 2021). And through measuring the serum THBS2 level of normal controls and patients, Jiang et al. confirm that THBS2 may be a biomarker for early diagnosis of NSCLC (Jiang et al., 2019). Therefore, we hypothesize that circ_0079530 regulates NSCLC cell function via miR-584-5p/THBS2 axis.

Accordingly, in this study, we investigated the effect and mechanism of circ_0079530 on the development of NSCLC.

Materials and methods

Patient samples

63 pairs of NSCLC and adjacent normal tissue specimens were enrolled in this study, which was permitted by Sichuan Science City Hospital. All patients who provided these samples had not received chemotherapy or radiation therapy previously, and each subject signed the written informed consent. After the operation, all tissue specimens were immediately frozen at -80°C until use.

Table 1. Primers sequences used for PCR.

Name		Primers for PCR (5'-3')
Circ_0079530	Forward	AAATAGATCCGGTGTCTAAATGC
	Reverse	TCCATTTTCTCCTTCTCTGGAA
TWIST1	Forward	CTCGGACAAGCTGAGCAAGA
	Reverse	GCTCTGGAGGACCTGGTAGA
miR-186-5p	Forward	GCCGAGCAAAGAATTCTCCT
	Reverse	CTCAACTGGTGTCGTGGAG
miR-576-5p	Forward	GCCGAGATTCTAATTTCTCC
	Reverse	CTCAACTGGTGTCGTGGAG
miR-580-3p	Forward	GCCGAGTTGAGAATGATGAA
	Reverse	CTCAACTGGTGTCGTGGAG
miR-584-5p	Forward	GCCGAGTTATGGTTTGCCTG
	Reverse	CTCAACTGGTGTCGTGGAG
THBS2	Forward	CTGGCTCTGTGGGTGTGG
	Reverse	TTGCTGAGGTCATCTGCGTT
GAPDH	Forward	AAGGCTGTGGGCAAGGTCATC
	Reverse	GCGTCAAAGGTGGAGGAGTGG
U6	Forward	CTCGCTTCGGCAGCACA
	Reverse	AACGCTTCACGAATTTGCGT

Cell culture

NSCLC cell lines (A549, H460, and NCI-H1299), human bronchial epithelial cells (16HBE), and HEK-293T cells were purchased from Procell (Wuhan, China). A549 cells were cultured in Ham's F12K (Procell), H460, NCI-H1299, and 16HBE cells were incubated in RPMI-1640 (Gibco, Thermo Fisher Scientific, Rockville, MD, USA), and HEK-293T cells were fostered in DMEM (Gibco) at 37°C with 5% CO_2. 10% fetal bovine serum (FBS; Gibco) and 1% penicillin/streptomycin (Gibco) was added to mediums.

Quantitative real-time PCR (qRT-PCR)

TRIzol Reagent (Invitrogen, Carlsbad, CA, USA) was used during total RNA extraction. Then, the RNA concentration was examined by NanoDrop One/OneC (Thermo Scientific, Shanghai, China), and Synthesis Kit (Invitrogen) was used to obtain cDNA. The cDNA was mixed with specific primers and SYBR Green (Solarbio, Beijing, China) to perform qRT-PCR. Relative expression was normalized by U6 small nuclear 1 (RNU6) or Glyceraldehyde-phosphate dehydrogenase (GAPDH) and calculated by the $2^{-\Delta\Delta CT}$ method. Primer sequences are shown in Table 1.

CircRNA characterization

RNA was lysed in Trigol (Dingguo Changsheng Biotech, Beijing, China). One portion of RNAs from A549 and NCI-H1299 cells was co-incubation to 3 U/μg RNase R (Geneseed, Guangzhou, China) or an equal volume of the 1×Reaction Buffer (Geneseed) for 30 min at 37°C. After RNase R treatment, the RNA expression was analyzed by qPCR. On the other side, 4 mg/mL actinomycin D (Sigma-Aldrich, St. Louis, MO, USA) or an equal volume of dimethylsulphoxide was added in cell culture mediums and the RNA of NSCLC cells was isolated to qRT-PCR.

Cell transfection

Cell transfection was adopted by using Lipofectamine 2000 (Invitrogen, Carlsbad, CA, USA). The short hairpin RNA or overexpression plasmid of circ_0079530 (sh-circ_0079530 or circ_0079530), miR-584-5p mimic or inhibitor (miR-584-5p or in-miR-584-5p), the small interfering RNA or pcDNA overexpression plasmid of THBS2 (si-THBS2 or THBS2), and their corresponding negative controls (sh-

NC, vector, miR-NC, in-miR-NC, si-con, pcDNA) were manufactured by Sangon Biotech Co., Ltd. (Shanghai, China).

Cell counting kit 8 (CCK8) assay

About 2×10^4 transfected NSCLC cells were cultured until the predetermined time points (0, 24, 48, and 72h). Then, 10 μL of CCK-8 reagent (Sigma) was added to each well. 4 hours later, the absorbance at 450 nm was measured by an enzyme immunoassay analyzer (Bio-Tek, Winooski, VT, USA).

Colony formation assay

Cell suspension with transfected cells was seeded in 6-well plates (200 cells per hole), and grown in an incubator for 2 weeks. Subsequently, the culture medium was removed. The cells were fixed with para-formaldehyde (Phygene, Fuzhou, China) and dyed with crystal violet (Phygene). Then, the number of colonies containing more than 50 cells was counted.

EdU staining

According to the instructions of the KeyFluor488 EdU Kit (keyGEN Biotech, Jiangsu, China), EdU staining was performed to evaluate cell proliferation. Briefly, differently transfected NSCLC cells were stained with EdU, Apollo, and DAPI solution. Finally, EdU-positive cells (%) were calculated via fluorescence images.

Flow cytometry

After being transfected, NSCLC cells were grown for 24h and harvested by centrifugation. Then, a commercial Annexin V-fluorescein isothiocyanate (FITC)/propidium iodide (PI) apoptosis analysis kit (Vazyme, Nanjing, China) was employed to stain cells. Finally, a flow cytometer (Thermo Fisher) was utilized to quantify apoptotic cells.

Transwell assays

24 wells of Transwell membranes were implemented to measure NSCLC cell migration and invasion. For cell migration detection, transfected cells suspended with the serum-free medium were pipetted over the upper chambers (5×10^4/well), and a culture medium with 10% FBS was pipetted into the bottom chambers. The difference between migration and invasion experiments lies in the upper chambers. In invasion assay, cells need to invade the Matrigel-coated polycarbonate transwell filter. 24h later, migrated or invaded cells were fixed with para-formaldehyde (Phygene) and dyed with 0.1% crystal violet (Phygene). Migrated and invaded cells were counted under a microscope (100×).

Table 2. The antibodies in western blotting and IHC.

Antibody	Cat.	Dilution ratio	Source
PCNA	ab92552	1:1000	Abcam (Cambridge, MA, USA)
Bax	ab32503	1:10000	Abcam
E-cadherin	20874-1-AP	1:10000	Proteintech
THBS2	ab112543	1:1000	Abcam
GAPDH	10494-1-AP	1:50000	Proteintech
ki67	ab15580	1:200	Abcam
Goat Anti-Rabbit IgG H&L (HRP)	ab6721	1:20000	Abcam

Western blot (WB) analysis

The tissues and cells were lysed by RIPA buffer (Beyotime, Shanghai, China) to obtain total protein. Then, the protein was separated by SDS-PAGE gel and transferred to PVDF membranes (Bio-Rad, Hercules, CA, USA). Afterward, the protein signals of the membranes were visualized by the BeyoECL Plus kit (Beyotime) after co-incubation with primary and secondary antibodies, presented in Table 2, at 4°C overnight. Image Lab software was used to analyze the gray value of proteins.

Bioinformatics analysis and dual-luciferase reporter system

StarBase, CircInteractome, and circBank online software were used to retrieve the miRNA binding sites in circ_0079530, and the retrieval results are shown in the Venn diagram. StarBase was used to predict miR-584-5p-binding sites in the functional gene THBS2. To generate luciferase reporter for circ_0079530 and THBS2, fragments of wild or mutant type circ_0079530 and wild or mutant type 3'UTR of THBS2 mRNA were cloned into the upstream of pmirGLO luciferase reporter. HEK-293T cells in 96-well plates were co-transfected with 100 ng above reporter vectors and 1 nM miRNA mimics. Dual-Lumi™ II Luciferase Assay Kit (Beyotime) was used to measure the luciferase activities after transfection for 48h.

RIP assay

Magna RIP Kit (Millipore, Billerica, MA, USA) was utilized in this part. Firstly, cells were treated with RIP lysis buffer. Then, cell lysates were mixed with magnetic beads pre-coated with antibodies against Ago2 or IgG. The enrichment of circ_079530 and miR-584-5p was detected by qRT-PCR.

Xenograft model

5-week-old male BALB/c nude mice were purchased from Vital River Laboratory (Beijing, China), and this animal study was authorized by the Animal Ethics

Committee of Sichuan Science City Hospital. NCI-H1299 cells transfected with sh-NC or sh-circ_0079530 were subcutaneously inoculated into the dorsal side of the mice (n=5/group). Tumor volume was firstly calculated on the 5th day after cell injection, and the length (L) and width (W) of the forming tumors were measured every 4 days. The volume (V) of the nodules was assessed according to the formula: V (mm^3) = ($L \times W^2$)/2. After 27-d inoculation, tumors were taken out and weighed.

Immunohistochemistry (IHC) assay

IHC assay was performed as described (Huang et al., 2017). In brief, paraffin-embedded tissues were cut into 4-μm thickness. Then, serial sections of tissue were incubated with antibodies (Table 2) at 4°C overnight and then with secondary antibodies for 1h at room

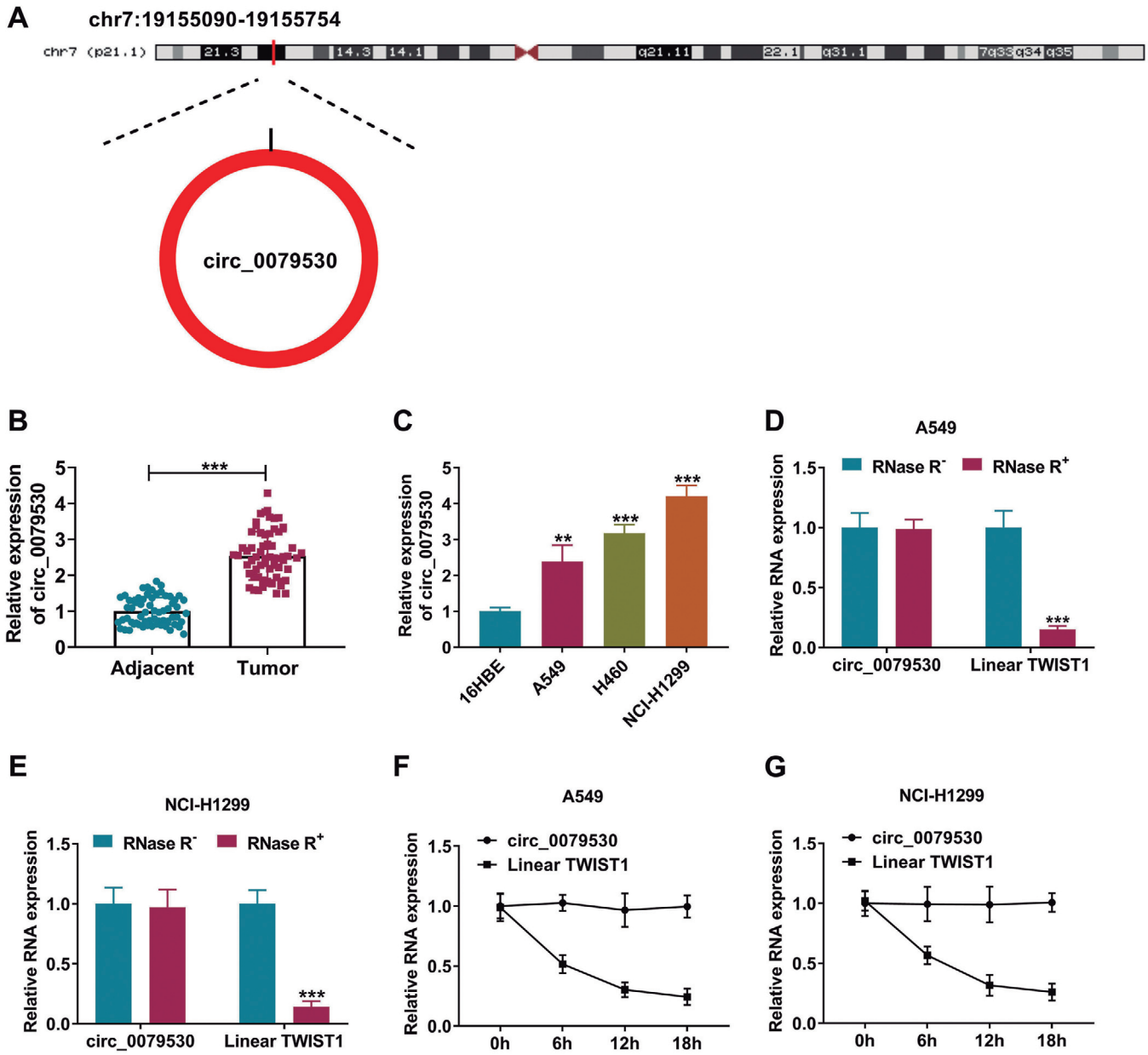

Fig. 1. Circ_0079530 is highly expressed in NSCLC tissues and cells. **A.** The chromosomal location of circ_0079530 was shown. **B, C.** The expression of circ_0079530 was measured by qRT-PCR analysis in 63 pairs of NSCLC tissues and adjacent normal tissues, as well as in NSCLC cells and normal 16HBE cells. **D-G.** The circular characteristic of circ_0079530 was assessed by RNase R assay **(D-E)** and Actinomycin D assay **(F-G)** in A549 and NCI-H1299 cells. ***P*<0.01, ****P*<0.001.

temperature.

Statistical analysis

Data were presented as the mean ± SD. The comparison was tested by unpaired t-test (two-tailed) and 1/2-way analysis of variance (ANOVA). Tukey's or Sidak's multiple comparisons test was performed after ANOVA. The correlations between circ_0079530, miR-584-5p, and THBS2 were analyzed using Pearson correlation analysis. Statistical analyses were carried out using GraphPad Prism 8.0 software. A value of $P<0.05$ was considered to be significant.

Results

Circ_0079530 was overexpressed in NSCLC tissues and cells

Circ_0079530 is located at chr7: 19155090-19155754 and is formed by the back-splicing of the TWIST1 gene (Fig. 1A). In the tumor tissues of NSCLC patients, we found that circ_0079530 expression was higher than that in adjacent normal tissues (Fig. 1B). Moreover, circ_0000808 expression was also higher in three NSCLC cell lines (A549, H460, and NCI-H1299) than that in 16HBE cells (Fig. 1C). Besides, RNase R

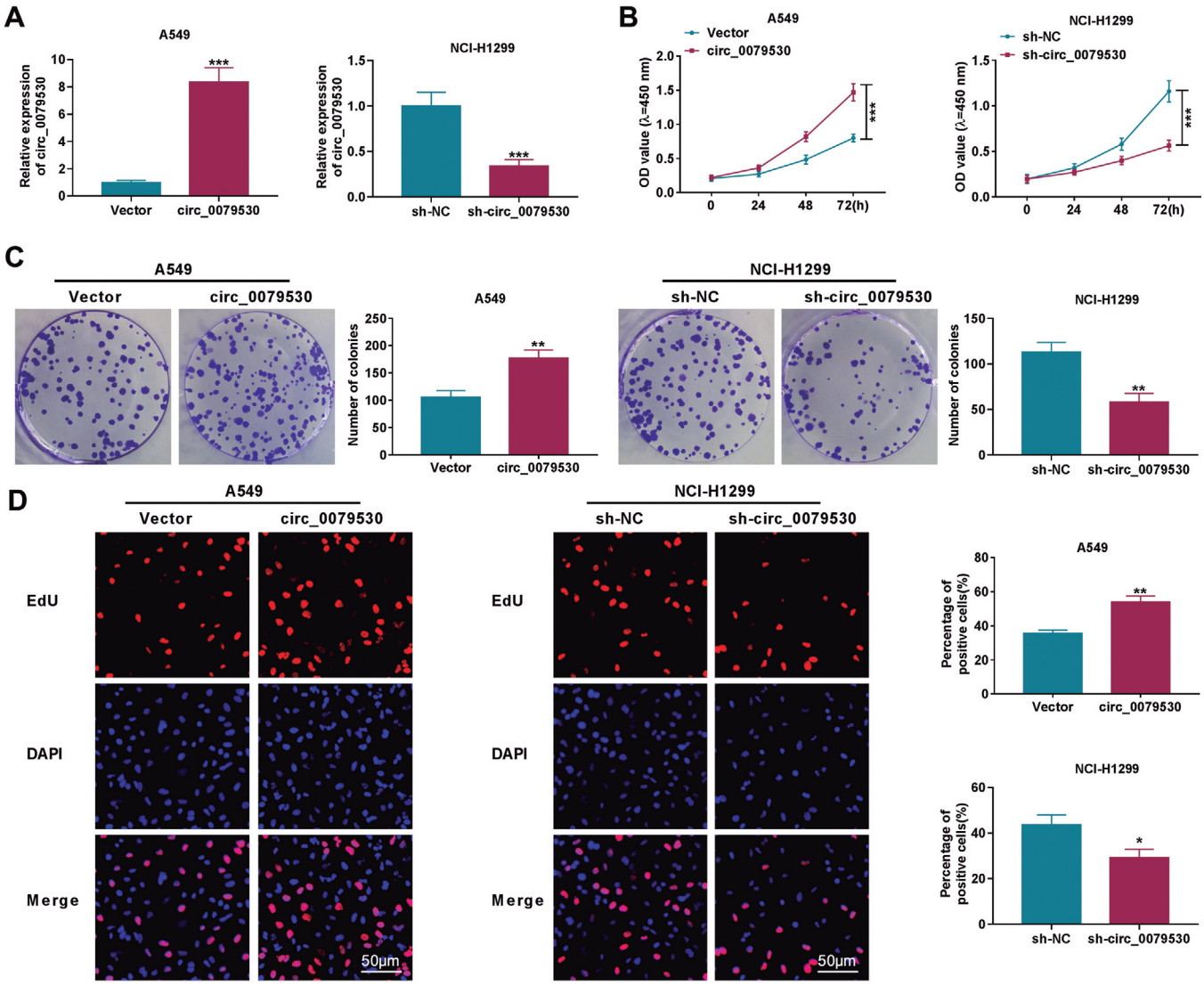

Fig. 2. Circ_0079530 promotes NSCLC cell proliferation *in vitro*. The circ_0079530 overexpression plasmid was transfected into A549 cells and sh-circSLC7A5 was transfected into NCI-H1299 cells. **A.** The expression of circ_0079530 was measured by qRT-PCR analysis. **B-D.** The cell proliferation was assessed by CCK-8 assay **(B)**, colony formation assay **(C)** and EdU staining assays **(D)**. **P*<0.05, **P<0.01, ****P*<0.001.

digestion and actinomycin D treatment had little effect on circ_0079530 expression, while its linear RNA TWIST1 was sharply reduced (Fig. 1D-G). These data confirmed that circ_0079530, a circular RNA, was upregulated in NSCLC tissue and cells, which might play an important role in the development of NSCLC.

Circ_0079530 facilitated NSCLC cell proliferation and motility and inhibited cell apoptosis.

In order to figure out the influences of circ_0000745 on cell function, circ_0000745 was overexpressed in A549 cells and knocked down in NCI-H1299 cells. Circ_0000745 expression was significantly upregulated in A549 cells transfected with circ_0079530 and reduced in NCI-H1299 cells transfected with sh-circ_0079530 (Fig. 2A). CCK8 assay, colony formation assay, and EdU assay was used to measure NSCLC cell proliferation, and the results showed that overexpression of circ_0079530 markedly increased the viability, the colony numbers and the EdU positive cells of A549 cells, and circ_0079530 inhibition caused a decrease in the viability, the colony numbers and the EdU positive cells of NCI-H1299 cells (Fig. 2B-D). On the contrary, the upregulated circ_0079530 obviously repressed A549 cell apoptosis, but the silencing of circ_0079530 promoted the apoptosis of NCI-H1299 cells (Fig. 3A). In addition, the number of migrated and invaded cells of A549 cells was facilitated by circ_079530 overexpression, while circ_0079530 inhibition hindered

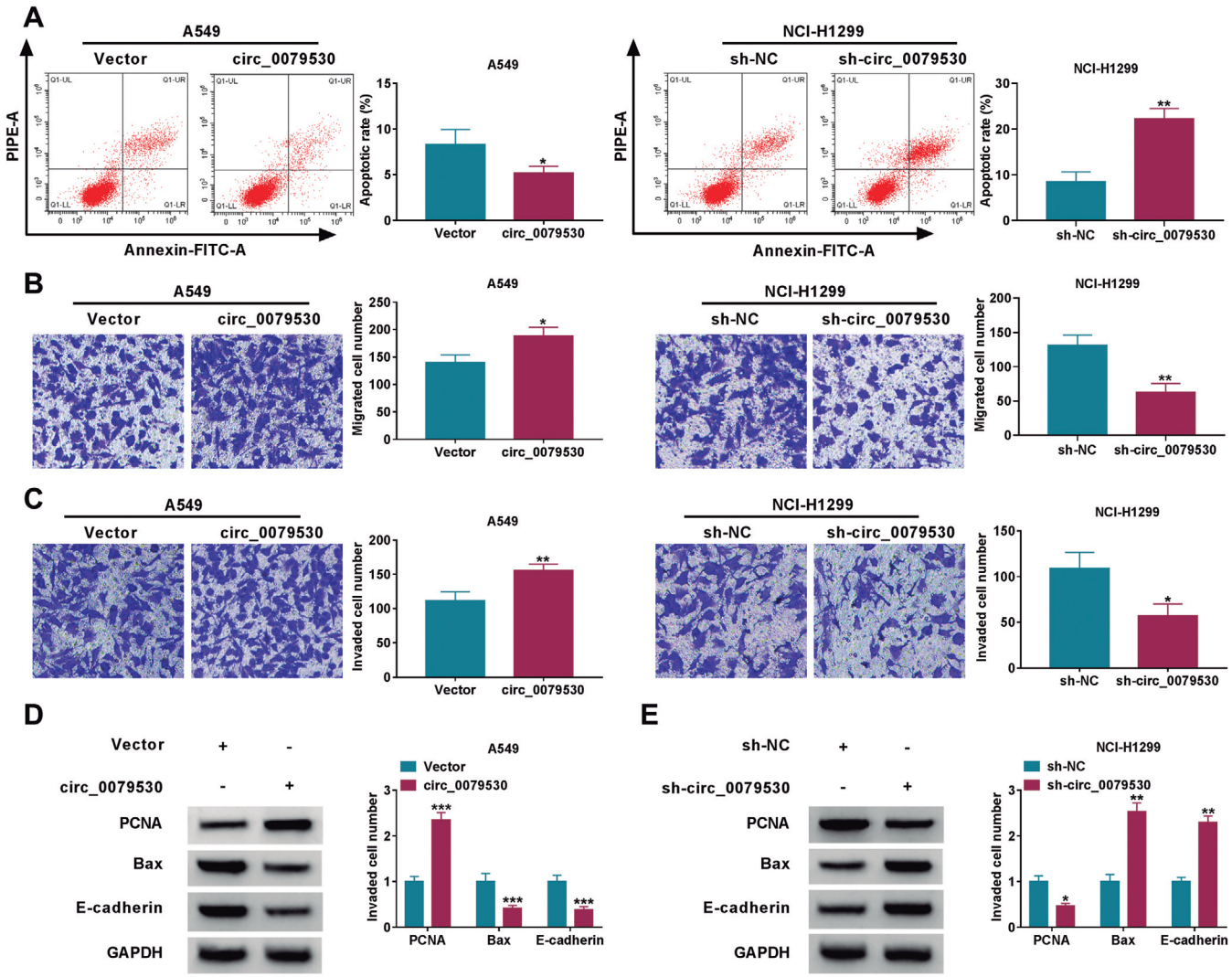

Fig. 3. Circ_0079530 inhibits NSCLC cell apoptosis, and boosted migration and invasion *in vitro*. A549 cells were transfected with circ_0079530 overexpression plasmid and NCI-H1299 cells were transfected with sh-circSLC7A5. **A.** Cell apoptosis was measured by flow cytometry assay. **B, C.** The cell migration and invasion were examined by transwell assays. **D, E.** The protein levels of PCNA, Bax and E-cadherin were detected by Western blot analysis. *P<0.05, **P<0.01, ***P<0.001.

the migration and invasion of NCI-H1299 cells (Fig. 3B,C), confirming that circ_0079530 can promote NSCLC cell metastasis. Moreover, ectopic circ_0079530 expression elevated the protein level of PCNA and downregulated the protein level of Bax and E-cadherin in A549 cells (Fig. 3D). Conversely, circ_0079530 knockdown decreased the protein level of PCNA and increased the protein level of Bax and E-cadherin in NCI-H1299 cells (Fig. 3E). Thus, all results manifested that circ_0079530 might act as an oncogene in NSCLC.

Circ_0079530 physically interacted with miR-584-5p via target binding

Four miRNAs were predicted as potential targets of circ_0079530 by three online websites (Fig. 4A) and compared with adjacent tissues There are two miRNAs including miR-186-5p and miR-584-5p that were remarkably downregulated in 6 randomly selected NSCLC tumor tissues (Fig. 4B). Meanwhile, miR-186-5p and miR-584-5p expression levels were markedly repressed after being transfected with circ_0079530 in A549 cells (Fig. 4C). After silencing circ_0079530 in NCI-H1299 cells, the expression levels of miR-186-5p and miR-584-5p were significantly increased (Fig. 4D). Considering that miR-584-5p had a higher response to changes in circ_0079530 expression levels, we chose miR-584-5p for follow-up research. To further examine this target relationship, the predicted binding sites of miR-584-5p were mutated in circ_0079530 (Fig. 4E), and miR-584-5p mimic evidently decreased the luciferase activity of circ_0079530 WT reporter vector, whereas it had no influence on that of circ_0079530 MUT vector in HEK-293T cells (Fig. 4F). RIP assay displayed that the enrichment of circ_0079530 and miR-584-5p with Ago2 was higher than IgG (Fig. 4G,H).

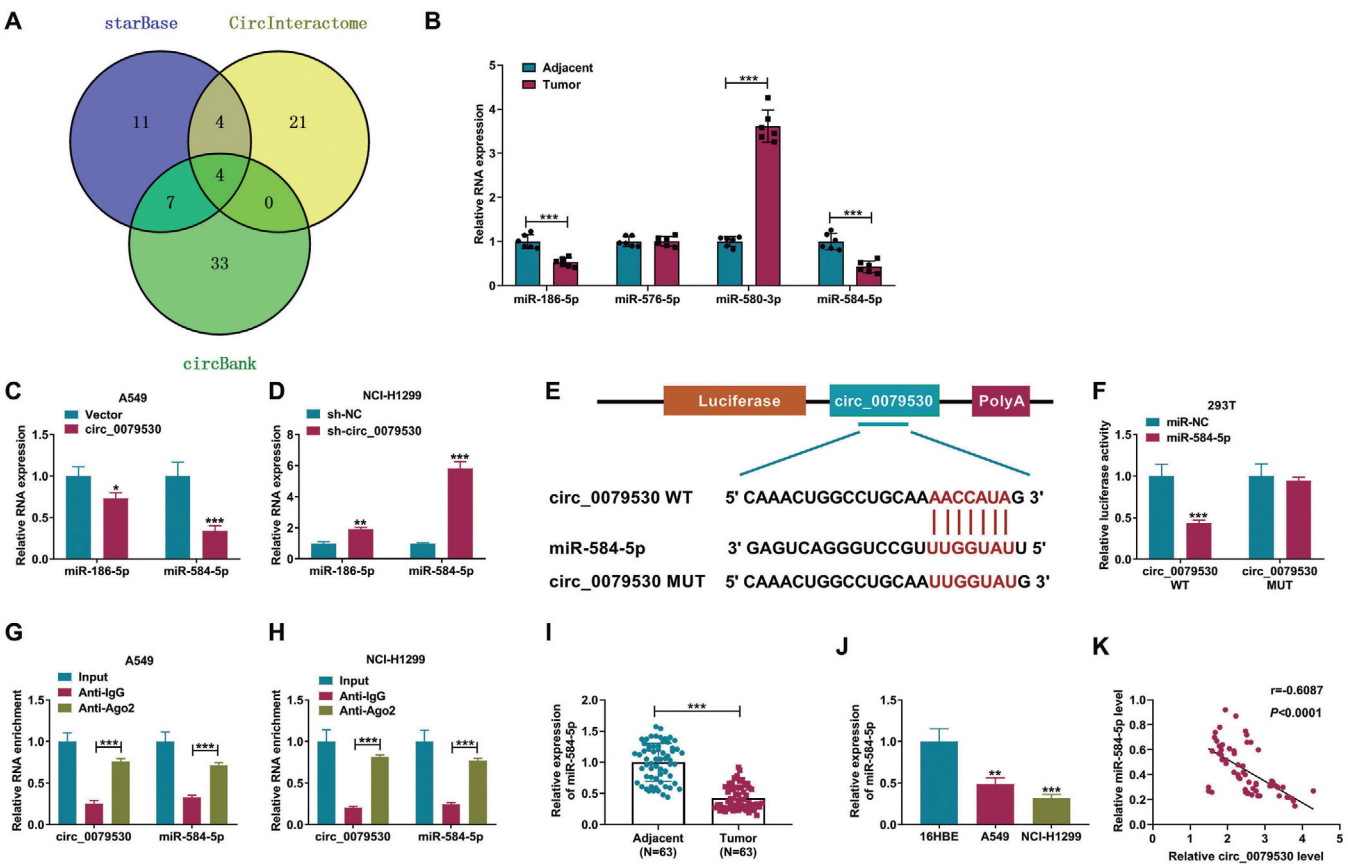

Fig. 4. MiR-584-5p is a target of circ_0079530. **A.** Venn diagram shows the number of miRNAs that were predicted as targets for circ_0079530 in starBase, CircInteractome and circBank online software. **B.** The expression of miR-186-5p, miR-576-5p, miR-580-3p and miR-584-5p were determined by qRT-PCR analysis in 6 pairs of randomly selected adjacent and tumor tissues. **C, D.** The expression of miR-186-5p and miR-584-5p were examined by qRT-PCR analysis in A549 cells transfected with circ_0079530 and NCI-H1299 cells transfected with sh-circ_0079530. **E.** The binding sites of miR-584-5p and circ_0079530 are shown. **F.** The luciferase activity was detected by dual-luciferase reporter assay in HEK-293T cells co-transfected with circ_0079530 WT or circ_0079530 MUT and miR-584-5p or miR-NC, respectively. **G, H.** qRT-PCR analysis and RIP assays were performed to detect miR-584-5p and circ_0079530 expression in A549 and NCI-H1299 cells. **I, J.** The expression of circ_0079530 was measured by qRT-PCR analysis in 63 pairs of NSCLC tissues and adjacent normal tissues, as well as in 16HBE, A549 and NCI-H1299 cells. **K.** Correlation between miR-584-5p and circ_0079530 expression in NSCLC tissues was analyzed by Pearson correlation coefficient. **P*<0.05, ***P*<0.01, ****P*<0.001.

Next, the expression of miR-584-5p was measured in NSCLC patients' tissues and cells, and the results showed that miR-584-5p was obviously downregulated in NSCLC tumor tissues and cells (Fig. 4I,J). Pearson's correlation analysis revealed that there was a negative correlation between the expression of circ_0079530 and miR-584-5p (Fig. 4K). Collectively, the above results indicated that circ_0079530 acted as a sponge of miR-584-5p in NSCLC.

The functional regulation of circ_0102273 on NSCLC progression might be reversed by miR-584-5p

For further examinations, miR-584-5p and in-miR-584-5p were respectively constructed and transfected into A549 and NCI-H1299 cells, and the results confirmed that miR-584-5p obviously increased the expression of miR-584-5p in A549 cells, and in-miR-584-5p markedly decreased the expression of miR-584-5p in NCI-H1299 cells (Fig. 5A). After co-transfected circ_0079530 and miR-584-5p or sh-circ_0079530 and in-miR-584-5p, cell biological function was measured. MiR-584-5p mimic weakened the promoting effect of circ_009530 overexpression on A549 cell proliferation, but in-miR-584-5p ameliorated the inhibitory effect of circ_0079530 knockdown on NCI-H1299 cell proliferation (Fig. 5B-D). Also, the inhibition of circ_0079530 on A549 cell apoptosis was attenuated by miR-584-5p, while the promotion of sh-circ_0079530 on NCI-H1299 cell apoptosis was overturned by in-miR-

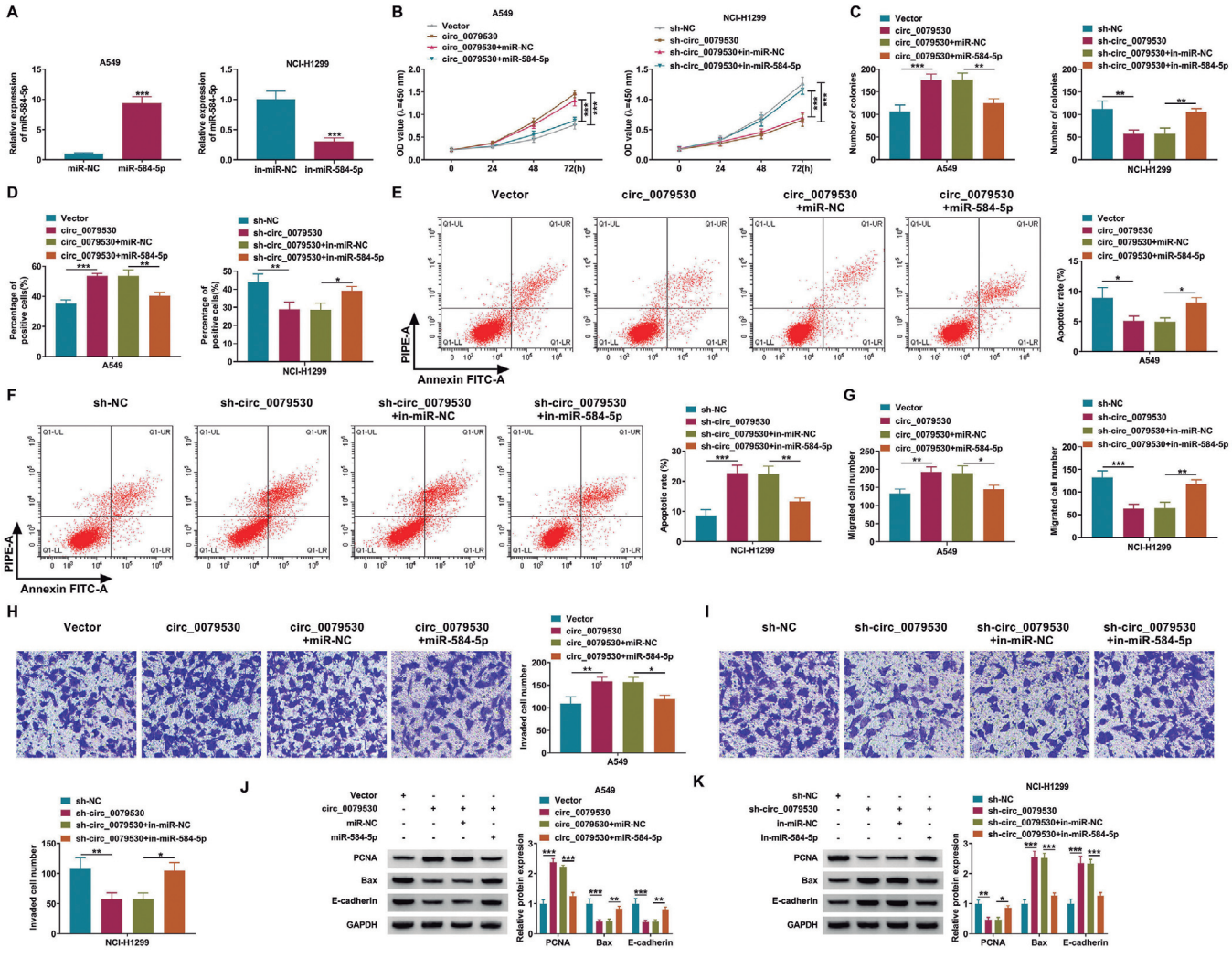

Fig. 5. Circ_0079530 promotes NSCLC cell growth *in vitro* via regulating miR-584-5p. **A.** The expression of miR-584-5p in A549 cells transfected with miR-NC or miR-584-5p and NCI-H1299 cells transfected with in-miR-NC or in-miR-584-5p was measured by qRT-PCR analysis. **B-K.** circ_0079530 and miR-584-5p were co-transfected into A549 cells and sh-circ_0079530 and in-miR-584-5p were co-transfected into NCI-H1299 cells. **B-D.** Cell proliferation was assessed by CCK-8 assay **(B)**, colony formation assay **(C)** and EdU staining **(D)**. **E, F.** Cell apoptosis was measured by flow cytometry assay. **G-I.** Cell migration and invasion were examined by transwell assays. **J, K.** The protein levels of PCNA, Bax and E-cadherin were detected by Western blot analysis. **P*<0.05, ***P*<0.01, ****P*<0.001.

584-5p (Fig. 5E,F). Moreover, circ_0079530 distinctly enhanced cell migration and invasion of A549 cells, while miR-584-5p mimic rescued this effect. In NCI-H1299 cells, sh-circ_0079530 notably suppressed cell migration and invasion, but this effect was reverted by a miR-584-5p inhibitor (Fig. 5G-I). In addition, increased miR-584-5p abolished circ_0079530 upregulation-mediated influences on the protein levels of PCNA, Bax, and E-cadherin in A549 cells. Meanwhile, in-miR-584-5p regained circ_0079530 silence-mediated influences on the protein levels of PCNA, Bax, and E-cadherin in NCI-H1299 cell (Fig. 5J,K).

MiR-584-5p directly targeted THBS2

Subsequently, StarBase was used to predict the target of miR-584-5p, and the results showed that the conserved binding sites of miR-584-5p might complementally bind with the 3'UTR of THBS2 mRNA (Fig. 6A). Then, we found that miR-584-5p inhibited THBS2 expression, and in-miR-584-5p increased THBS2 expression (Fig. 6B,C). In HEK-293 T cells, miR-584-5p significantly suppressed the luciferase activity of the THBS2 3'UTR WT luciferase reporter vector but had a slight influence on the THBS2 3'UTR MUT luciferase reporter vector (Fig. 6D). Furthermore, both miR-584-5p and THBS2 mRNA were massively enriched on the beads incubated with Ago2 (Fig. 6E,F). All these data indicated that there was a binding relationship between miR-584-5p and THBS2. Next, the mRNA and protein expression of THBS2 was detected, and data showed that THBS2 expression was upregulated in NSCLC tissues and cells (A549 and NCI-H1299) compared with adjacent normal tissues and 16HBE cells (Fig. 6G-J). Also, we found that circ_0079530 increased THBS2 protein expression, but overexpression of miR-584-5p was able to restore this effect (Fig. 6K). Also, sh-circ_0079530 repressed THBS2 protein expression, while knockdown miR-584-5p counteracted the influence (Fig. 6L). In addition, the correlation analysis between THBS2 and miR-584-5p or circ_0079530 was performed. Fig. 5M,N exhibited that

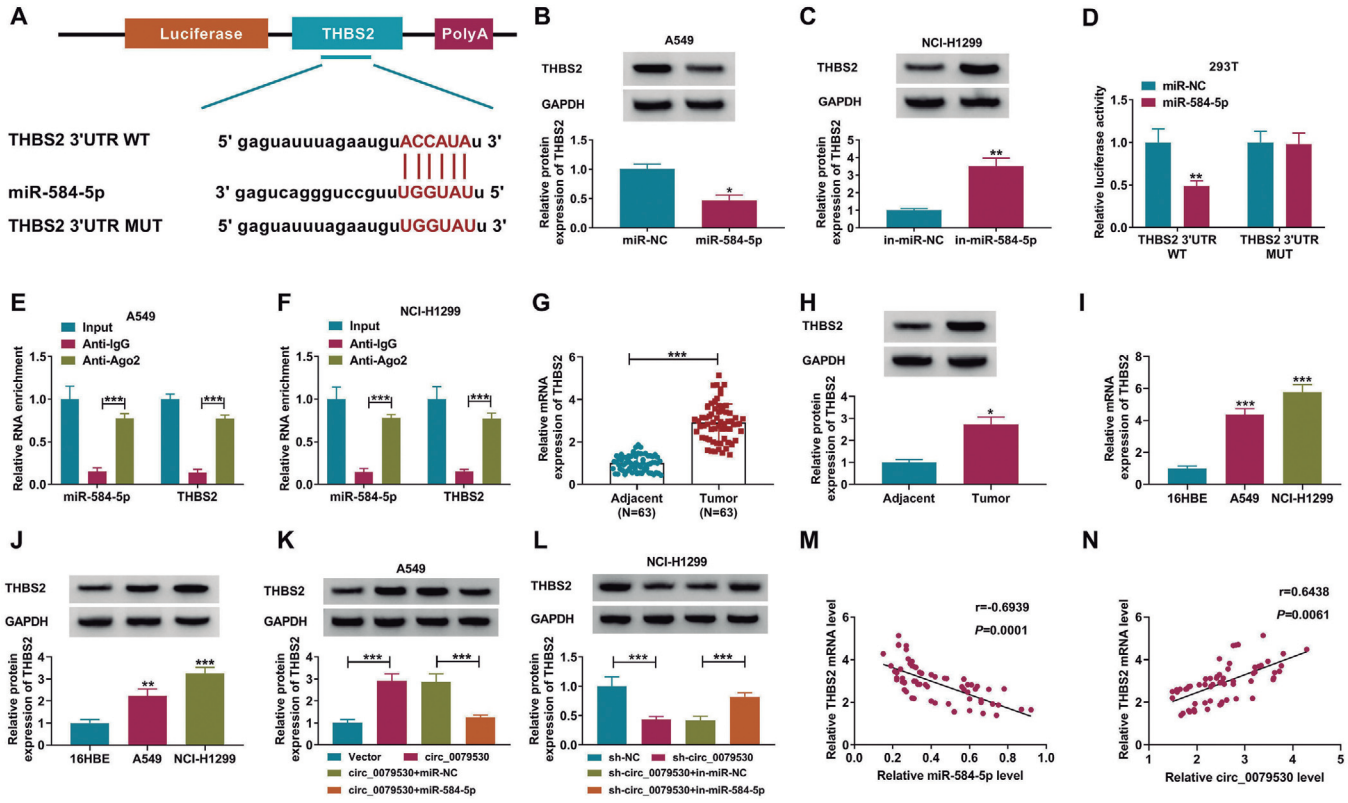

Fig. 6. Circ_0079530 indirectly regulates THBS2 expression via sponging miR-584-5p. **A.** The binding sites of miR-584-5p and THBS2 3'UTR are shown. **B, C.** The relative expression of THBS2 was detected by Western blot analysis in miR-584-5p-overexpressed A549 cells and miR-584-5p-silenced NCI-H1299 cells. **D.** The luciferase activity was measured by dual-luciferase reporter assay in HEK-293T cells co-transfected with THBS2 3'UTR WT or THBS2 3'UTR MUT and miR-584-5p or miR-NC, respectively. **E, F.** qRT-PCR analysis and RIP assays were performed to examine miR-584-5p and THBS2 expression in A549 and NCI-H1299 cells. **G-J.** The expression of THBS2 was measured by qRT-PCR and Western blot in NSCLC tissues and adjacent normal tissues, as well as in 16HBE, A549 and NCI-H1299 cells. **K, L.** THBS2 protein expression was detected by Western blot in A549 and NCI-H1299 cells. **M, N.** Correlation of THBS2 mRNA and miR-584-5p or circ_0079530 expression in NSCLC tissues was analyzed by Pearson correlation coefficient. **P*<0.05, ***P*<0.01, ****P*<0.001.

THBS2 was negatively correlated with miR-584-5p and positively correlated with circ_0079530, suggesting that circ_0079530 might regulate THBS2 expression by miR-584-5p.

MiR-584-5p regulated NSCLC progression by targeting THBS2

To confirm that miR-584-5p regulated NSCLC cell malignancy by targeting THBS2, we transfected miR-584-5p or in-miR-584-5p into NSCLC cells to upregulate or downregulate miR-584-5p expression. Also, sh-THBS2 or THBS2 overexpression vector was transfected into NSCLC cells to induce the silence and overexpression of THBS2 (Fig. 7A,B). Subsequently, we found that the obvious promotion of in-miR-584-5p on A549 cell proliferation was reversed after co-transfecting with sh-THBS2. And the inhibition of miR-584-5p on NCI-H1299 cell proliferation was reversed after co-transfecting with THBS2 (Fig. 7C-E). Besides, miR-584-5p inhibitor and miR-584-5p mimic respectively reduced and increased the apoptosis cell rate in A549 and NCI-H1299 cells, but these effects were rescued by THBS2 silence and THBS2 upregulation in turn (Fig. 7F,G). For cell metastasis ability, the data showed that the knockdown of THBS2

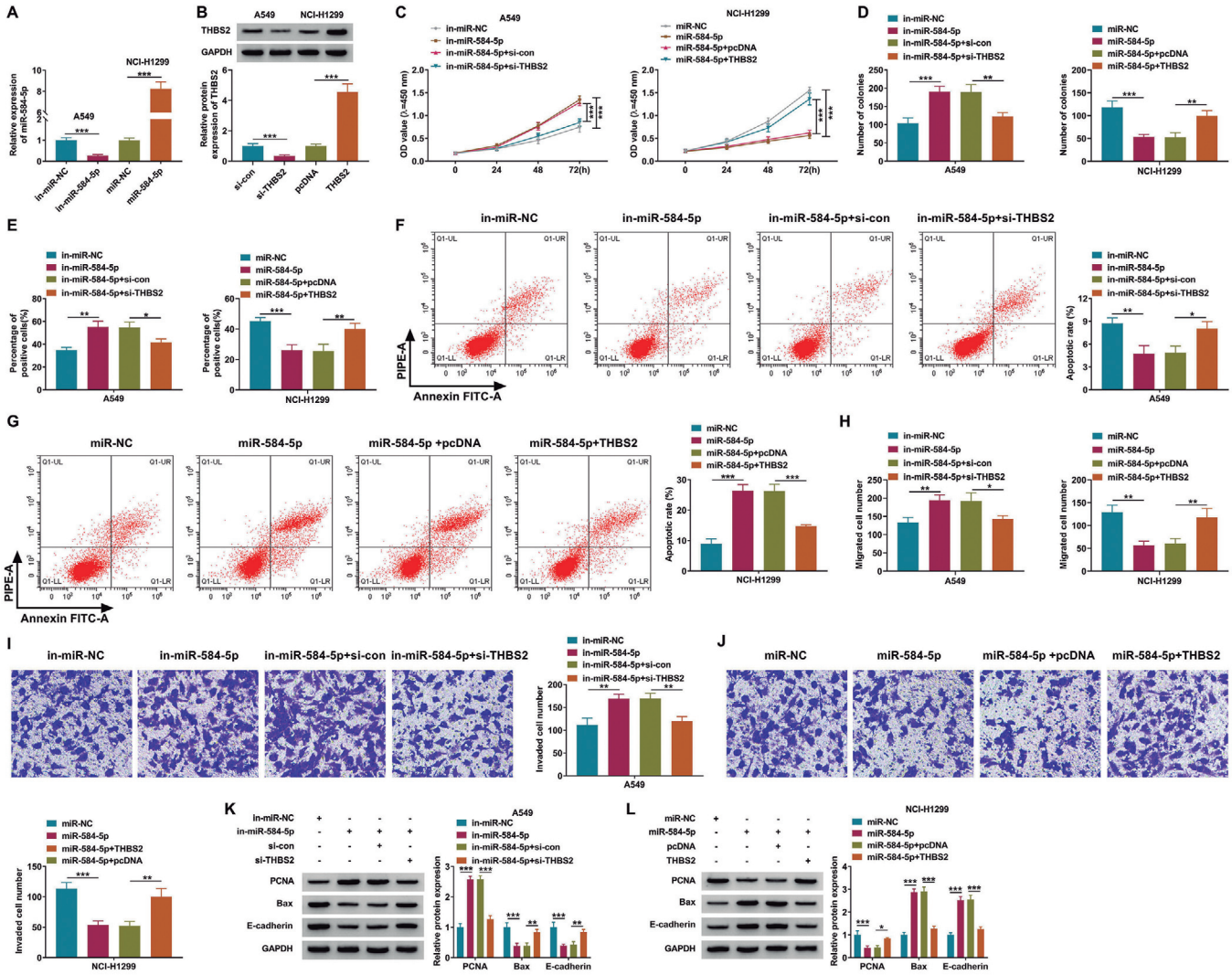

Fig. 7. MiR-584-5p suppresses NSCLC cell growth *in vitro* via targeting THBS2. **A.** The expression of miR-584-5p in A549 cells transfected with in-miR-NC or in-miR-584-5p and NCI-H1299 cells transfected with miR-NC or miR-584-5p was measured by qRT-PCR analysis. **B.** The THBS2 expression in A549 cells transfected with si-con or si-THBS2 and NCI-H1299 cells transfected with pcDNA or THBS2 was detected by Western blot analysis. **C-L.** in-miR-584-5p and si-THBS2 were co-transfected into A549 cells, and miR-584-5p and THBS2 were co-transfected into NCI-H1299 cells. **C-E.** cell proliferation was assessed by CCK-8 assay **(C)**, colony formation assay **(D)** and EdU staining **(E)**. **F, G.** Cell apoptosis was measured by flow cytometry assay. **H-J.** Cell migration and invasion were examined by transwell assays. **K, L.** The protein levels of PCNA, Bax and E-cadherin were detected by Western blot analysis. **P*<0.05, ***P*<0.01, ****P*<0.001.

abated the promoting influence of miR-584-5p silence on cell migration and invasion, but the overexpression of THBS2 counteracted the inhibiting effect of miR-584-5p mimic on cell migration and invasion (Fig. 7H-J). Furthermore, we found that in-miR-584-5p was able to regulate the levels of function-related proteins (PCNA, Bax, and E-cadherin) in A549 cells, but sh-THBS2 greatly restored these effects. In contrast, miR-584-5p mediated influences on the levels of function-related proteins (PCNA, Bax, and E-cadherin) in NCI-H1299 cells were reverted by THBS2 (Fig. 7K,L). Taken together, miR-584-5p regulated NSCLC cell proliferation, apoptosis, and metastasis via modulating THBS2 expression.

Interference of circ_0079530 inhibited NSCLC tumorigenesis in vivo

In order to investigate the effect of circ_0079530 silence on the formation and growth of xenograft tumors, NCI-H1299 cells transfected with sh-NC or sh-circ_0079530 were injected into nude mice. Through constructing a mouse model, we found that sh-circ_0079530 significantly inhibited the tumor size and weight when compared with the sh-NC group (Fig. 8A-C). Additionally, the results showed that circ_0079530 and THBS2 expression were repressed and miR-584-5p expression was promoted in the tumor tissues of the sh-circ_0079530 group (Fig. 8D,E). Also, the protein level of PCNA was downregulated, while the protein levels of Bax and E-cadherin were upregulated after circ_0079530 knockdown (Fig. 8F). Meanwhile, the IHC assay confirmed that the positive cells of THBS2, ki-67, and PCNA were reduced, whereas the Bax and E-cadherin positive cells were increased in the tumor tissues of the sh-circ_0079530 group compared to the sh-NC group (Fig. 8G).

Discussion

NSCLC is one of the leading causes of tumor-related deaths in the world (Bray et al., 2018). Due to hidden

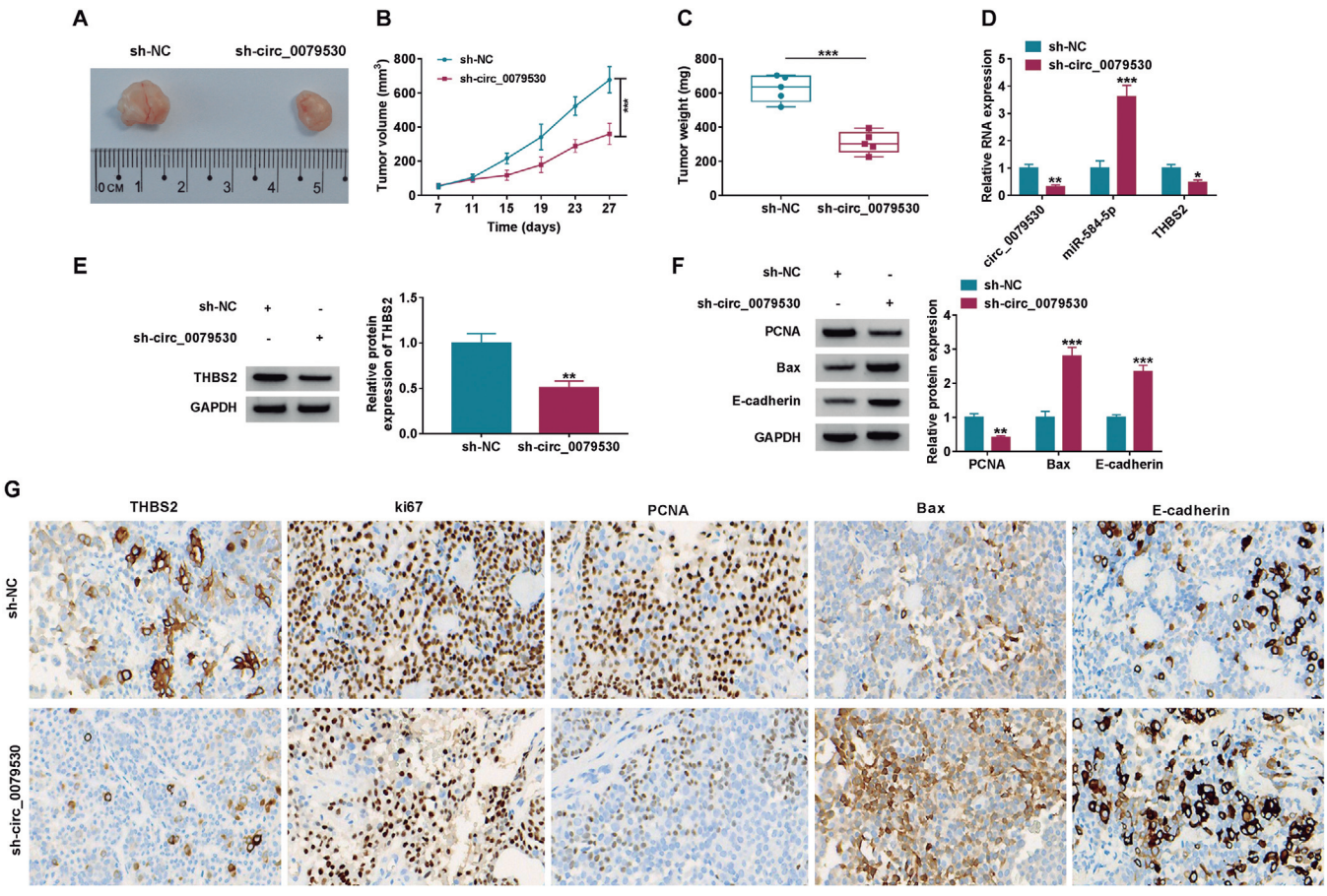

Fig. 8. Silencing of circ_0079530 represses NSCLC tumor growth *in vivo*. **A, B.** The *in vivo* growth curve and representative images of xenografts. **C.** The weight at the end points of xenografts. **D.** The expression of circ_0079530, miR-584-5p and THBS2 mRNA were determined by qRT-PCR analysis in xenografts of each group. **E, F.** The protein expression of THBS2 **(E)**, PCNA, Bax and E-cadherin **(F)** were detected by Western blot. **G.** The positive cells of THBS2, ki67, PCNA, Bax and E-cadherin were examined by IHC staining in xenografts of each group. **P*<0.05, ***P*<0.01, ****P*<0.001.

onset, most patients are already at an advanced stage with lymph node metastasis or distant metastasis when they are diagnosed (Gridelli et al., 2015; Duma et al., 2019). Although new therapies have better treatment of NSCLC, the 5-year survival rate is only about 16% (Kumar et al., 2021). The discovery and research of possible biomarkers and mechanisms are expected to provide new ideas for the clinical treatment of NSCLC.

CircRNA, highly conserved and stable in structure, may become effective diagnostic biomarkers for a variety of cancers, including NSCLC (Wang et al., 2020b). Therefore, the exploration of circRNA expression and regulation mechanism of NSCLC has become one of the research hotspots. With the deepening of research, the pro-cancer and anti-cancer roles of some circRNAs have been revealed in the progress of NSCLC. For instance, circSLC25A16 promoted NSCLC progression and glycolysis by absorbing miR-488-3p to release the inhibition of the HIF-1α/LDHA axis (Shangguan et al., 2020). Circ_0002483 contributed to its target genes (GRB2, FOXO1, and FOXO3) expression and repressed the ability of proliferation, invasion, and the Taxol resistance of NSCLC cells via targeting miR-182-5p (Li et al., 2019). Circ_0026134 silencing restrained cell growth and invasion by miR-1256 and miR-1287 (Chang et al., 2019). In this work, we found that circ_0079530 was highly expressed in NSCLC tissues and cells, and knocking down circ_0079530 inhibited the growth and metastasis of NSCLC cells, which were consistent with the results of previous studies (Li et al., 2018). The difference was that we had further proved the effect of circ_0079530 in NSCLC cells through overexpression of circ_0079530.

Subsequently, we explored miRNAs that could bind to circ_0079530. According to the prediction of the bioinformatics websites and the screening of cell experiments, miR-584-5p was used as a candidate miRNA of circ_0079530. Previous studies had verified that miR-584-5p played a role in promoting or suppressing cancer progression in various cancers, such as NSCLC, hepatocellular carcinoma, glioblastoma, and gastric cancer (Li et al., 2017; Zhang et al., 2020; Cao et al., 2021; Lee et al., 2021). Research about NSCLC and miR-584-5p had shown that miR-584-5p was a worthy tumor suppressor, and regulated the malignant biological behavior of NSCLC cells by negatively regulating the mRNA expression of target genes (Ma et al., 2020; Lee et al., 2021). Consistent with these, our experiment results confirmed that miR-584-5p expression was lower in NSCLC tissues and cells than in the controls. Also, it is negatively correlated with the expression of circ_0079530. In addition, the effects of overexpression and knockdown of circ_0079530 on the growth, apoptosis, and motility of NSCLC cells can be respectively reversed by miR-584-5p mimic and inhibitor. The above evidence indicated that miR-877-5p may be the target miRNA of circ_0079530.

THBS2, a member of the thrombospondin family, is a glycoprotein that can mediate the interactions of cell-to-cell and cell-to-matrix. The protein was obviously upregulated in cancer specimens when in contrast with the control specimens and plays an important role in colorectal carcinoma (Qian et al., 2019) and gastric cancer (Deng et al., 2021). Weng et al. found that the mRNA of THBS2 was overexpressed in a number of datasets of NSCLC (Weng et al., 2016). Moreover, THBS2 had both anti-angiogenic and oncogenic functions in the progression of NSCLC (Weng et al., 2016). Liu et al. demonstrated that THBS2 was able to facilitate lung cancer cell metastasis by inducing the upregulation of matrix metalloproteinase-13 (Liu et al., 2018). In addition, circ_0020123 contributed to THBS2 expression to promote cell proliferation and inhibited cell apoptosis via sponging miR-590-5p in NSCLC cells (Wang et al., 2020a). These facts illustrate that THBS2 might be used as a diagnostic and prognostic biomarker, and the clinical values of THBS2 in tumors remain to be further revealed. In this study, THBS2 was predicted and proved as a novel target of miR-584-5p in NSCLC cells. The regulation of miR-584-5p overexpression or inhibition in NSCLC progression was greatly attenuated by THBS2 upregulation or silence. We also found that circ_0079530 regulated the protein level of THBS2 by sponging miR-584-5p in NSCLC cells.

Considering the tumor-promoting effect of circ_0079530 in regulating the biological behaviors of NSCLC cells *in vitro*, we subsequently analyzed whether it had a similar effect in regulating the growth of xenograft tumors *in vivo*. The data revealed that circ_0079530 knockdown repressed xenograft tumor growth, at least partly by regulating miR-584-5p/THBS2 axis *in vivo*.

However, the specific molecular regulation mechanism of THBS2 in NSCLC cell proliferation, apoptosis, and metastasis has been not been studied yet due to experimental conditions and funding limitations. We will soon design a series of experiments for this problem, so as to elucidate the mechanism behind circ_0079530 modulating NSCLC.

In conclusion, our study proved a new hypothesis that circ_0079530 promoted the protein level of THBS2 and NSCLC malignant progression by negatively regulating miR-584-5p, which gave new insights into the molecular mechanism of NSCLC pathogenesis.

Data Availability Statement. Not applicable.

Conflicts of interest. The authors have no conflict of interest to declare.

Funding. None.

References

Bray F., Ferlay J., Soerjomataram I., Siegel R.L., Torre L.A. and Jemal A. (2018). Global cancer statistics 2018: GLOBOCAN estimates of incidence and mortality worldwide for 36 cancers in 185 countries. CA Cancer. J. Clin. 68, 394-424.

Cao Y., Wang F., Chen Y., Wang Y., Song H. and Long J. (2021). CircPITX1 regulates proliferation, angiogenesis, migration, invasion,

and cell cycle of human glioblastoma cells by targeting miR-584-5p/KPNB1 Axis. J. Mol. Neurosci. 71, 1683-1695.

Chang H., Qu J., Wang J., Liang X. and Sun W. (2019). Circular RNA circ_0026134 regulates non-small cell lung cancer cell proliferation and invasion via sponging miR-1256 and miR-1287. Biomed. Pharmacother. 112, 108743.

Deng L.Y., Zeng X.F., Tang D., Deng W., Liu H.F. and Xie Y.K. (2021). Expression and prognostic significance of thrombospondin gene family in gastric cancer. J. Gastrointest. Oncol. 12, 355-364.

Duma N., Santana-Davila R. and Molina J.R. (2019). Non-Small cell lung cancer: Epidemiology, screening, diagnosis, and treatment. Mayo. Clin. Proc. 94, 1623-1640.

Gridelli C., Rossi A., Carbone D.P., Guarize J., Karachaliou N., Mok T., Petrella F., Spaggiari L. and Rosell R. (2015). Non-small-cell lung cancer. Nat. Rev. Dis. Primers. 1, 15009.

Huang D.W., Huang M., Lin X.S. and Huang Q. (2017). CD155 expression and its correlation with clinicopathologic characteristics, angiogenesis, and prognosis in human cholangiocarcinoma. Onco. Targets. Ther. 10, 3817-3825.

Jiang Y.M., Yu D.L., Hou G.X., Jiang J.L., Zhou Q. and Xu X.F. (2019). Serum thrombospondin-2 is a candidate diagnosis biomarker for early non-small-cell lung cancer. Biosci. Rep. 39, BSR20190476.

Kumar V., Yadavilli S. and Kannan R. (2021). A review on RNAi therapy for NSCLC: Opportunities and challenges. Wiley. Interdiscip. Rev. Nanomed. Nanobiotechnol. 13, e1677.

Lee S.B., Park Y.S., Sung J.S., Lee J.W., Kim B. and Kim Y.H. (2021). Tumor suppressor miR-584-5p inhibits migration and invasion in smoking related non-small cell lung cancer cells by targeting YKT6. Cancers (Basel). 13, 1159.

Lee Y.T., Tan Y.J. and Oon C.E. (2018). Molecular targeted therapy: Treating cancer with specificity. Eur. J. Pharmacol. 834, 188-196.

Li S. and Han L. (2019). Circular RNAs as promising biomarkers in cancer: detection, function, and beyond. Genome. Med. 11, 15.

Li Q., Li Z., Wei S., Wang W., Chen Z., Zhang L., Chen L., Li B., Sun G., Xu J., Li Q., Wang L., Xu Z., Xia Y., Zhang D., Xu H. and Xu Z. (2017). Overexpression of miR-584-5p inhibits proliferation and induces apoptosis by targeting WW domain-containing E3 ubiquitin protein ligase 1 in gastric cancer. J. Exp. Clin. Cancer. Res. 36, 59.

Li J., Wang J., Chen Z., Chen Y. and Jin M. (2018). Hsa_circ_0079530 promotes cell proliferation and invasion in non-small cell lung cancer. Gene 665, 1-5.

Li X., Yang B., Ren H., Xiao T., Zhang L., Li L., Li M., Wang X., Zhou H. and Zhang W. (2019). Hsa_circ_0002483 inhibited the progression and enhanced the Taxol sensitivity of non-small cell lung cancer by targeting miR-182-5p. Cell Death. Dis. 10, 953.

Liang Z.Z., Guo C., Zou M.M., Meng P. and Zhang T.T. (2020). circRNA-miRNA-mRNA regulatory network in human lung cancer: an update. Cancer Cell. Int. 20, 173.

Liu J.F., Lee C.W., Tsai M.H., Tang C.H., Chen P.C., Lin L.W., Lin C.Y., Lu C.H., Lin Y.F., Yang S.H. and Chao C.C. (2018). Thrombospondin 2 promotes tumor metastasis by inducing matrix metalloproteinase-13 production in lung cancer cells. Biochem. Pharmacol. 155, 537-546.

Ma D., Qin Y., Huang C., Chen Y., Han Z., Zhou X. and Liu H. (2020). Circular RNA ABCB10 promotes non-small cell lung cancer progression by increasing E2F5 expression through sponging miR-584-5p. Cell Cycle 19, 1611-1620.

Panda A.C. (2018). Circular RNAs Act as miRNA Sponges. Adv. Exp. Med. Biol. 1087, 67-79.

Papatsirou M., Artemaki P.I., Karousi P., Scorilas A. and Kontos C.K. (2021). Circular RNAs: emerging regulators of the major signaling pathways involved in cancer progression. Cancers (Basel). 13, 2744.

Qian Z., Gong L., Mou Y., Han Y. and Zheng S. (2019). MicroRNA203a3p is a candidate tumor suppressor that targets thrombospondin 2 in colorectal carcinoma. Oncol. Rep. 42, 1825-1832.

Qin T., Li J. and Zhang K.Q. (2020). Structure, regulation, and function of linear and circular long non-coding RNAs. Front. Genet. 11, 150.

Santer L., Bar C. and Thum T. (2019). Circular RNAs: A novel class of functional RNA molecules with a therapeutic perspective. Mol. Ther. 27, 1350-1363.

Shangguan H., Feng H., Lv D., Wang J., Tian T. and Wang X. (2020). Circular RNA circSLC25A16 contributes to the glycolysis of non-small-cell lung cancer through epigenetic modification. Cell Death Dis. 11, 437.

Siegel R.L., Miller K.D. and Jemal A. (2018). Cancer statistics, 2018. CA. Cancer. J. Clin. 68, 7-30.

Wang Y., Xu R., Zhang D., Lu T., Yu W., Wo Y., Liu A., Sui T., Cui J., Qin Y., Dong Y., Leng X., Kong D., Du W., Huang Z., Su W., Yuan T., Sun X., Wang J. and Jiao W. (2019). Circ-ZKSCAN1 regulates FAM83A expression and inactivates MAPK signaling by targeting miR-330-5p to promote non-small cell lung cancer progression. Transl. Lung Cancer. Res. 8, 862-875.

Wang L., Zhao L. and Wang Y. (2020a). Circular RNA circ_0020123 promotes non-small cell lung cancer progression by sponging miR-590-5p to regulate THBS2. Cancer Cell. Int. 20, 387.

Wang X., Li H., Lu Y. and Cheng L. (2020b). Circular RNAs in human cancer. Front. Oncol. 10, 577118.

Weng T.Y., Wang C.Y., Hung Y.H., Chen W.C., Chen Y.L. and Lai M.D. (2016). Differential expression pattern of THBS1 and THBS2 in lung cancer: Clinical outcome and a systematic-analysis of microarray databases. PLoS One 11, e0161007.

Xu P., Wang L., Xie X., Hu F., Yang Q., Hu R., Jiang L., Ding F., Mei J., Liu J. and Xiao H. (2020). Hsa_circ_0001869 promotes NSCLC progression via sponging miR-638 and enhancing FOSL2 expression. Aging (Albany NY). 12, 23836-23848.

Xue M., Hong W., Jiang J., Zhao F. and Gao X. (2020). Circular RNA circ-LDLRAD3 serves as an oncogene to promote non-small cell lung cancer progression by upregulating SLC1A5 through sponging miR-137. RNA Biol. 17, 1811-1822.

Yang S.R., Schultheis A.M., Yu H., Mandelker D., Ladanyi M. and Buttner R. (2020). Precision medicine in non-small cell lung cancer: Current applications and future directions. Semin Cancer. Biol. 84, 184-198.

Zhang Y., Wang H., Li C., Gao L., Zheng Y., Chang W., Lu C. and Zhao X. (2020). CircSMYD4 regulates proliferation, migration and apoptosis of hepatocellular carcinoma cells by sponging miR-584-5p. Cancer Cell. Int. 20, 556.

Zhong Y., Du Y., Yang X., Mo Y., Fan C., Xiong F., Ren D., Ye X., Li C., Wang Y., Wei F., Guo C., Wu X., Li X., Li Y., Li G., Zeng Z. and Xiong W. (2018). Circular RNAs function as ceRNAs to regulate and control human cancer progression. Mol. Cancer 17, 79.

Accepted November 16, 2022